

PROCEEDINGS OF SPIE

[SPIDigitalLibrary.org/conference-proceedings-of-spie](https://spiedigitallibrary.org/conference-proceedings-of-spie)

Thermoelectrically-cooled extended-SWIR FPAs using unipolar barrier detectors

Michael MacDougal, Andrew Hood, Jeremy Thomas, Gary Wicks, Terry Golding, et al.

Michael MacDougal, Andrew Hood, Jeremy Thomas, Gary Wicks, Terry Golding, Edward K. Huang, "Thermoelectrically-cooled extended-SWIR FPAs using unipolar barrier detectors," Proc. SPIE 10624, Infrared Technology and Applications XLIV, 1062402 (9 May 2018); doi: 10.1117/12.2304388

SPIE.

Event: SPIE Defense + Security, 2018, Orlando, FL, United States

Thermoelectrically-cooled extended-SWIR FPAs using unipolar barrier detectors

Michael MacDougal, Andrew Hood, Jeremy Thomas

Attollo Engineering, LLC

Gary Wicks, Terry Golding

Amethyst Research, Inc.

Edward K. Huang

FLIR Systems, Inc.

ABSTRACT

Attollo Engineering will present results of our research program developing extended SWIR sensors as well as the packaging and camera electronics surrounding it. The 640x512 sensor uses GaInAsSb for the active layer and has a cutoff wavelength of 2.5 μm . The unipolar barrier structure enables a higher operating temperature by substantially reducing dark current caused by G-R mechanisms and surface leakage. The material is grown on GaSb and is made up of GaInAsSb absorber and contact layers separated by an AlGaSb barrier. We will present dark current and imaging results from the sensor fabrication at different temperatures. The detector array was hybridized to a 15 μm pixel pitch ROIC that has a direct injection unit cell. The hybridized sensor was packaged into a custom 4-stage thermoelectrically cooled package. The package was particularly designed to minimize the heat load and maximize the thermal conduction. We will present the trades that went into designing the package and the internals of the package. The cooler stabilized the sensor temperature at 200K. The electronics used to drive the package have the ability to change biases and timing on the fly using software controls. Attollo designed these electronics to be a low-cost solution for demonstrating sensors in many different modes. We will show information regarding each stage of integration and show the results of the imaging using the eSWIR sensor and supporting equipment.

Keywords: SWIR, FPA, Infrared, SLS

INTRODUCTION

Much short wavelength infrared (SWIR) research has been focused on the wavelength regime from 0.9 – 1.67 μm , primarily due to the availability of InGaAs, whose cutoff is 1.67 μm . However, the full SWIR band extends up to 2.5 μm , as shown in Figure 1, leaving much more phenomenology to be studied.

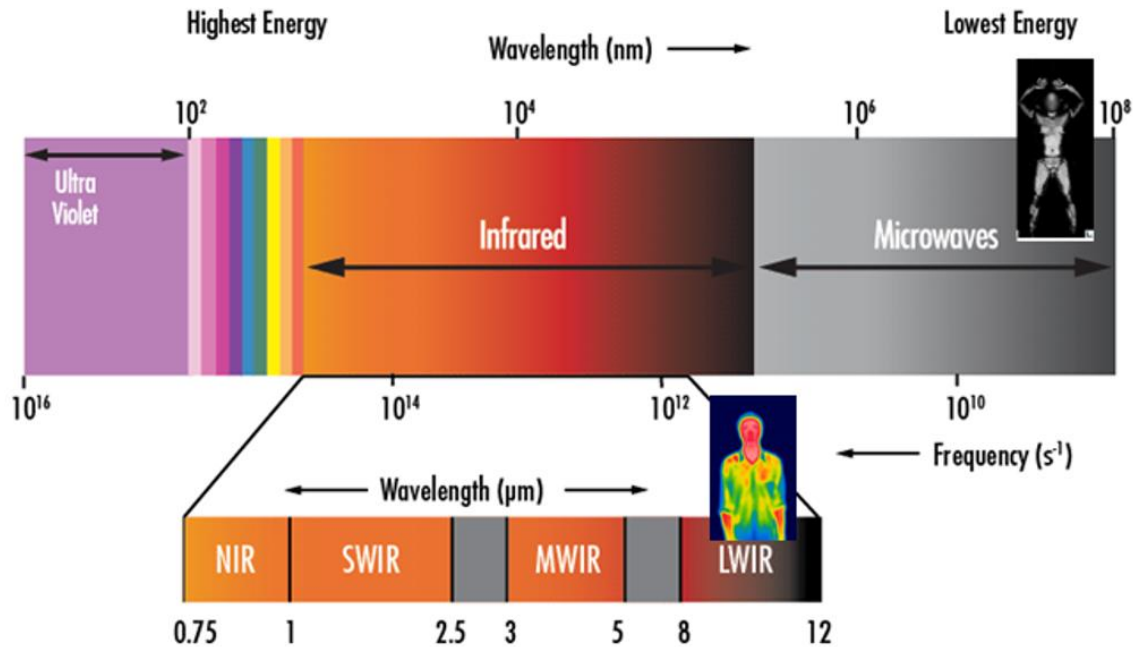


Figure 1 - Plot of electromagnetic spectrum showing the full SWIR spectrum (courtesy Thales).

This other part of the SWIR region we are calling the extended SWIR or eSWIR. Applications for this regime include hyperspectral imaging, agriculture, plastics sorting, astronomy, gas sensing, and defense applications. To extend the cutoff wavelength, the bandgap of the absorbing material must decrease. The downside to reducing the bandgap is that it causes the dark current to increase substantially, so much so that the sensor requires cooling. In this paper, we discuss our approach to designing an eSWIR device as well as an associated package without resorting to a cryocooler. Our intent is to make an eSWIR sensor that can be cooled by a thermoelectric cooler (TEC).

DEVICE DESIGN AND FABRICATION

Our first step is to use a material that can operate at a TEC-attainable temperature. Our target temperature is 200K, and then choose our material from there. The options for device materials are:

1. Strained InGaAs
2. HgCdTe
3. InGaAsSb

Our criteria for device choice is III-V material and lattice-matched because that is where our experience resides. The third option meets those criteria. Within this category, there are three options, as shown in Figure 2. The options are bulk P-I-N, bulk nBn, and strained layer superlattice (SLS) nBn. Our group chose the nBn structures because they have little to no depletion region, and this reduces the generation-recombination (G-R) current that can increase dark current.

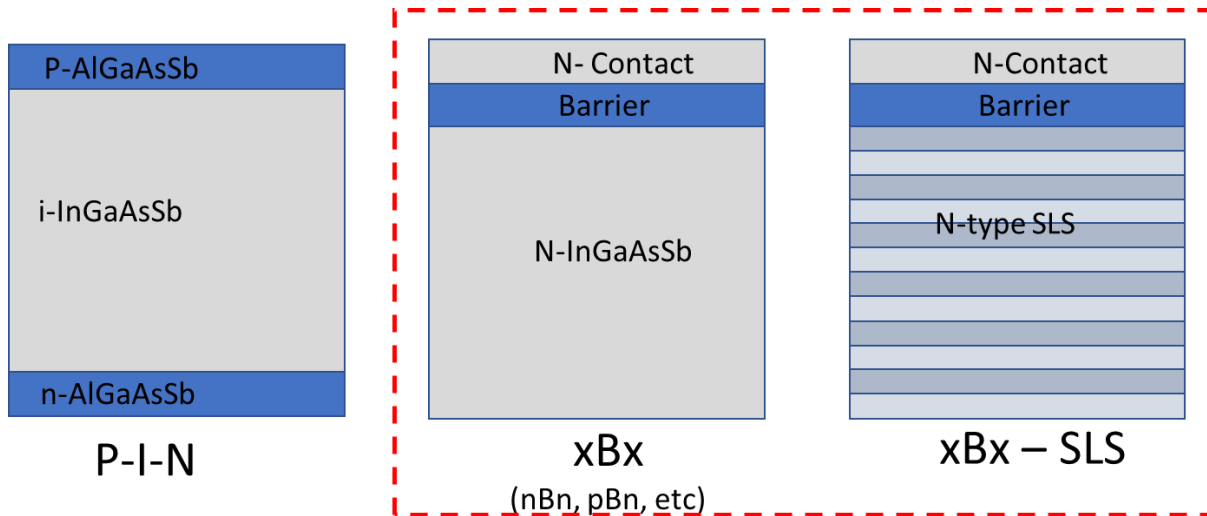


Figure 2 - Diagrams of potential InGaAsSb-based eSWIR detection structures

Bulk nBn structures were grown by Amethyst Research and SLS nBn structures were grown by Attollo Engineering.

Amethyst Structures

The Amethyst devices were grown using molecular beam epitaxy (MBE) on 3" GaSb substrates. Three structures were grown by Amethyst, with the different structures having different cutoff wavelengths:

1. 1.9 μm
2. 1.9 μm and 2.25 μm
3. 2.25 μm

The intent of the second structure is to use two different absorption regions with the shorter cutoff taking the bulk of the thickness of the total overall absorption material. The longer wavelength cutoff region is used for seeing bright phenomenology, whereas the thicker shorter wavelength cutoff material is used to take advantage of the night glow areas. In this way, we can see longer wavelength signals without the dark current penalty normally associated with the longer wavelength material. Spectral response measurements were taken to determine the penalty associated with this type of structure, shown in Figure 3.

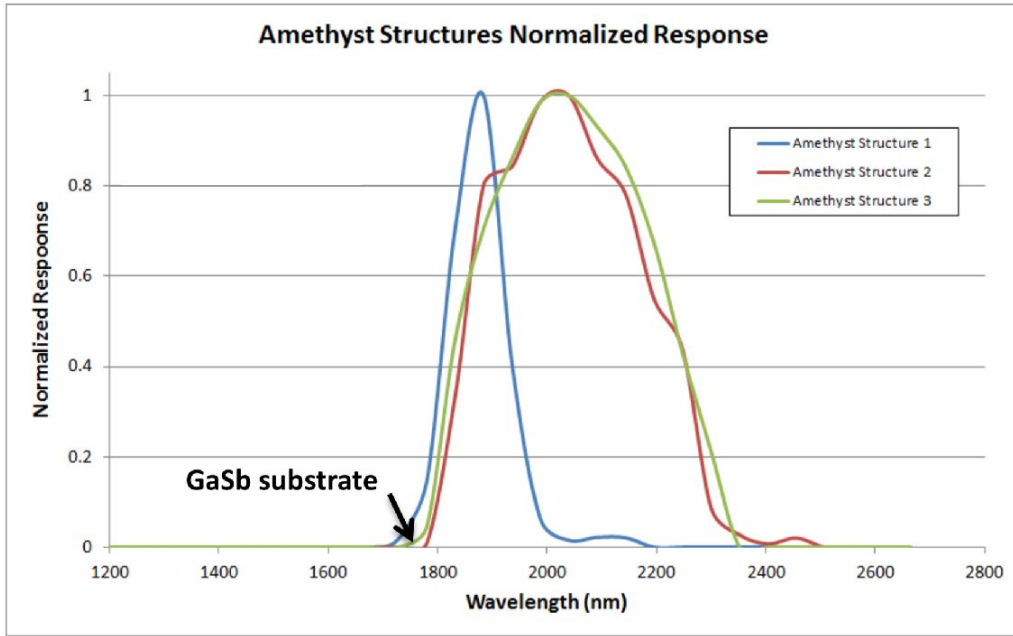


Figure 3 - Graph of spectral response of the different structures. Structure 2 and Structure 3 have similar response, indicating that the thin long wavelength material provided nearly identical response as a thick layer of the longer wavelength material.

The spectral response of Structures 2 and 3 are very similar, indicating that the thin material layer in Structure 2 provides nearly the same amount of response as Structure 3, which has a thick layer of longer wavelength material. The thin layer should contribute a much lower amount of dark current than the thick layer. Dark current measurements were taken from structures 1 and 2 (shown in Figure 4) and they are very similar, also indicating that the thin 2.25 μm cutoff layer has a minor affect on dark current. Therefore, this structure (Structure 2) gives the benefit of longer wavelength response, while suffering little penalty of higher dark current.

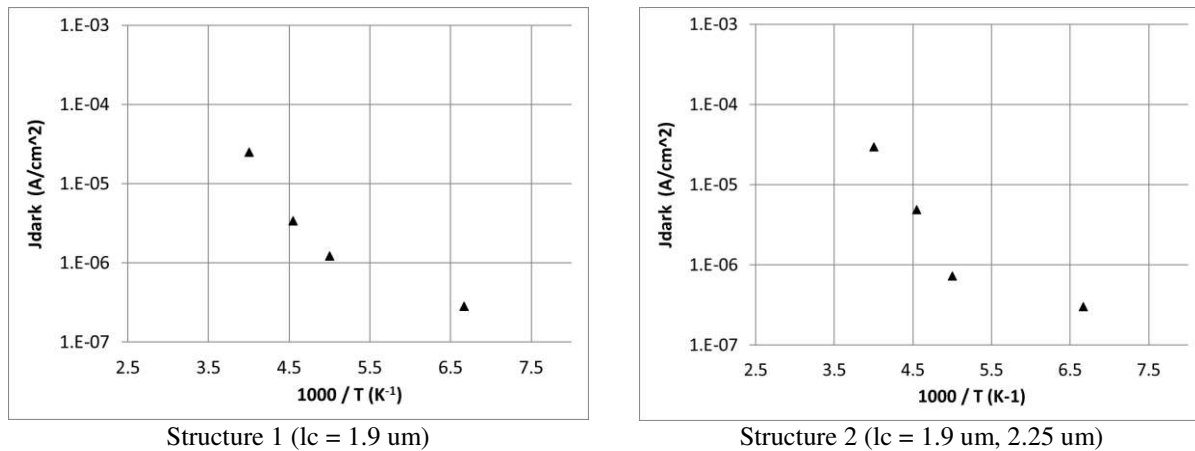


Figure 4 - Plots of dark current density as a function of temperature

Dark current was also measured on single element devices and compared against the empirical '07 rule¹. Figure 5 shows that the data is within 2x of the '07 rule, and therefore of good quality.

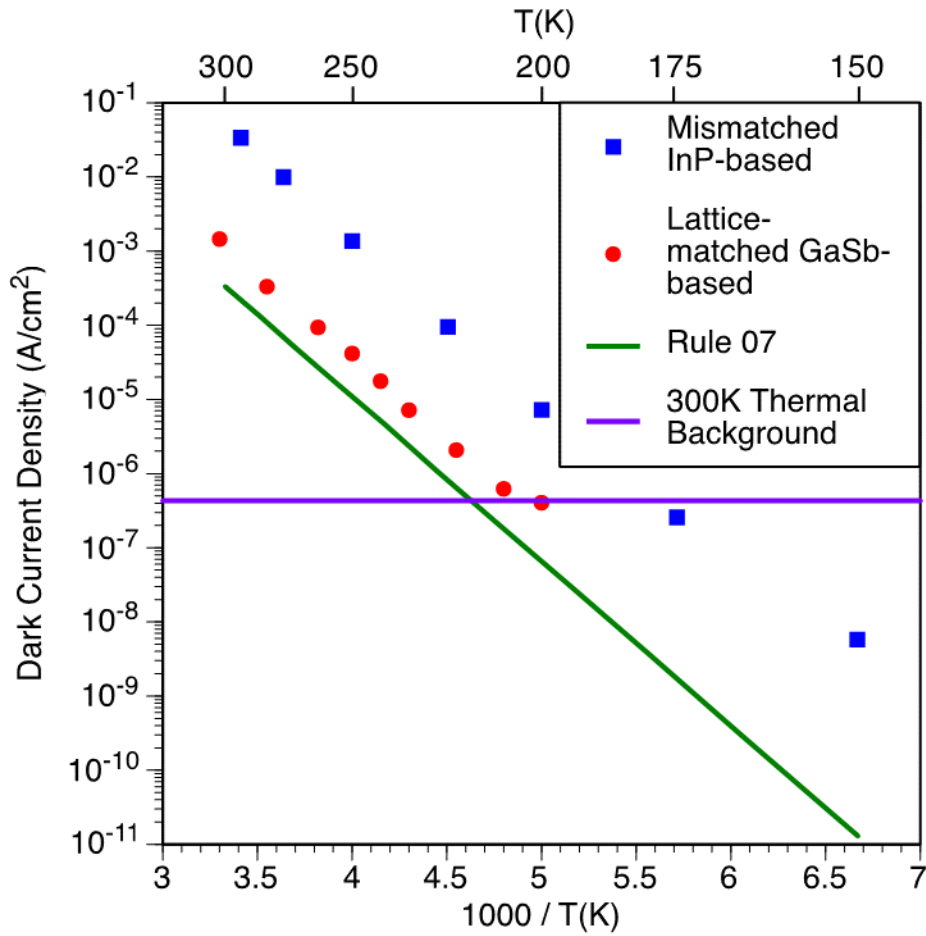


Figure 5 - Graph of dark current density vs reciprocal temperature showing close adherence to Rule '07.

Attollo Structures

Attollo grew an nBn SLS structure that has a cutoff of 2.5 μm . The samples were processed into test structures and characterized for spectral response and dark current. The spectral response at 293K is shown in Figure 6.

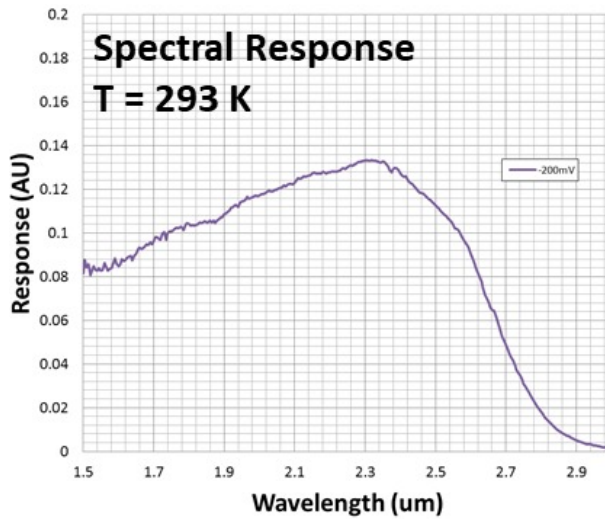


Figure 6 - Plot of spectral response as a function of wavelength, showing a cutoff of 2.65 um at 293K. The cutoff should shift to ~2.5 um at 160K.

The dark current at different temperatures is shown in Figure 7. The dark current at 170K is very close to the values for the 2.25 um cutoff material shown in Figure 6.

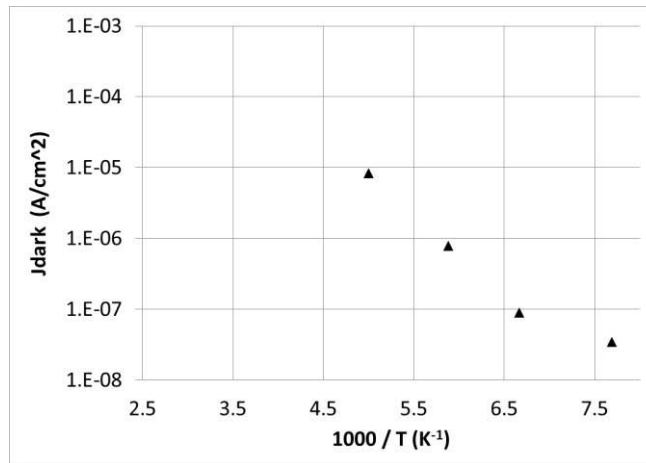


Figure 7 - Dark current versus 1000/T for Attollo structures with cutoff wavelength of 2.5 um

FPA FABRICATION

We continued processing the Amethyst structures into focal plane arrays (FPAs). The FPA is made up of the detector material discussed above and the readout integrated circuit (ROIC). With the dark current here, we chose a ROIC that had a large well capacity, in this case the FLIR ISC0403. The specs for this ROIC are shown in Table 1

Table 1 - ISC0403 ROIC Parameters

Parameter	Value
Format	640 x 512
Pixel Pitch	15 μm
Well size	6.3 Me-
Read noise	< 715 e-
Max full frame rate	120 fps

Dark current maps were taken of structure 1 to obtain information about uniformity. These maps were taken at different temperatures and are shown in Figure 8.

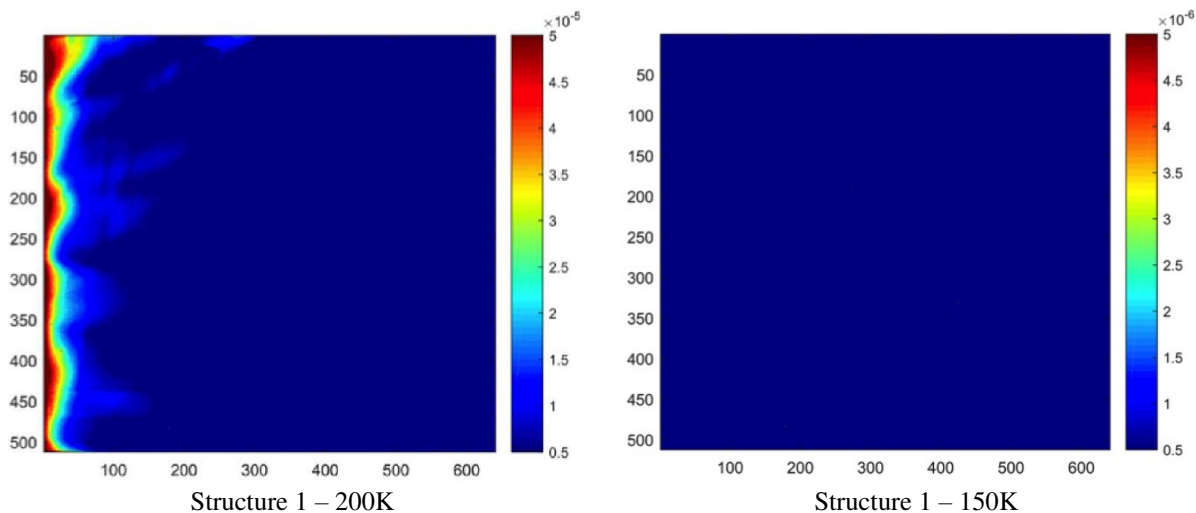


Figure 8 - Dark current density maps at different temperatures

The maps show uniform dark current density with some edge effects beginning to occur at 200K. Structure 2 was put into a LN₂-cooled dewar with a lens and used for outdoor imaging. Figure 9 shows the results. The only correction is a single-point offset correction. The result shows few outages and little nonuniformity.



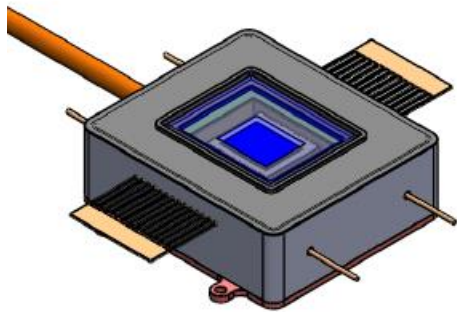
Figure 9 - Picture taken with sensor in LN₂ pour fill dewar heated to 200K.

The device design and fabrication portion of this project resulted in parts that performed well near 200K. The next step is to design and fabricate thermoelectric packages that can maintain these temperatures.

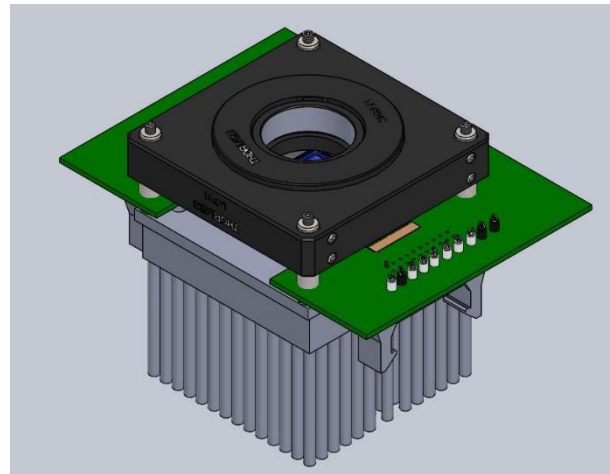
PACKAGING DESIGN

To achieve a ΔT of 100°C or more requires careful design. The thermal interfaces must have low resistance, the solar loading must be limited where possible, and sensor must be insulated from the sides of the dewar. We designed a vacuum package from the ground up. We used a 4-stage cooler and chose metals that were very thermally conductive. In addition, the connectors were selected to come out the side instead of the bottom of the package to improve heat flow.

We chose a vacuum package with pinch-off tube construction to insulate the sensor and the top of the TE cooler from the ambient temperature sides of the package. In order to reduce the thermal load on the top stage of the TEC, we used a “warm” shield that we connected to the lowest TEC stage in order to shunt the solar loading to the most efficient stage. A screen shot of the solid model is shown in Figure 10a. To remove the heat from the package, a heat sink is needed. We chose a large commercially available heat sink with a fan to remove the heat. A screen shot of the model with the heat sink is shown in Figure 10b.



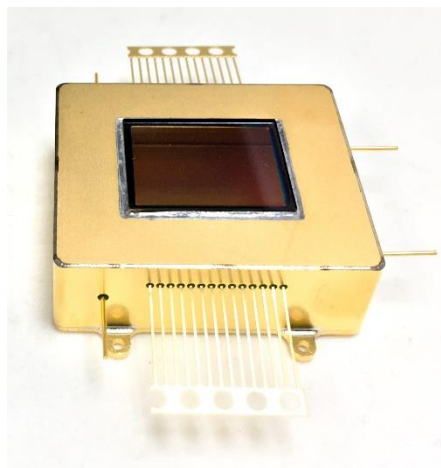
(a) Solid model of package



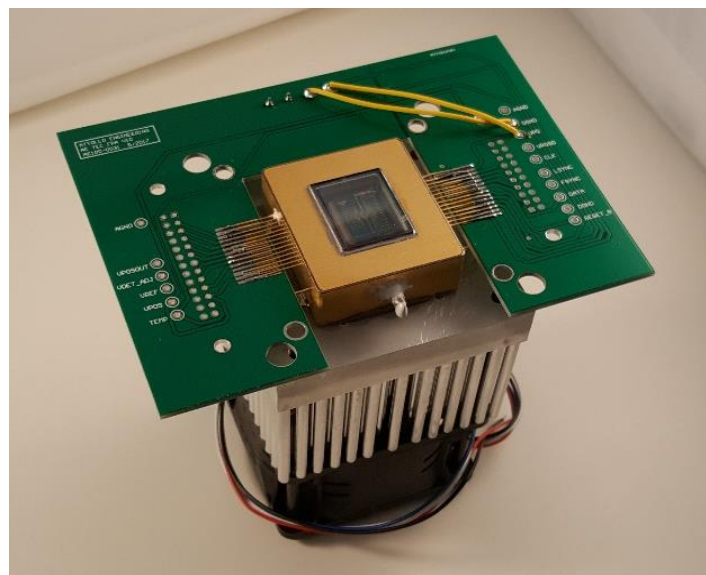
(b) Solid model of full assembly

Figure 10 - Screenshot of package solid model

After the package was designed, the parts were ordered and the packages was fabricated. The resulting package is shown in Figure 11a, and the full assembly with board and heat sink is shown in Figure 11b.



(a) Picture of assembled package

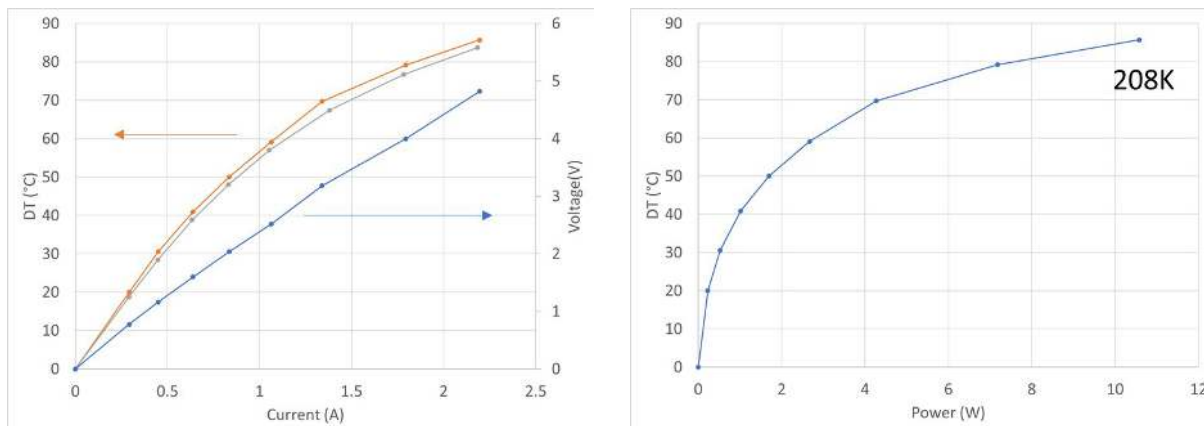


(b) Picture of package assembly with heat sink

Figure 11 - Pictures of package

As part of characterization of the package, we measured the temperature drop as a function of current and power input. Figure 12a shows the temperature drop with the sensor on and off. At a current of 2.2A, were able to achieve a temperature drop of 85°C. From our room temperature of 293°C, that gave us a working temperature of 208K. The

current was limited by the feedthroughs to < 2.25 A. However, the TEC can handle up to 5A, and therefore it is capable of lower temperatures. At 208K, the power being used by the cooler is 10.7W, shown in Figure 12b.



(a) Temperature drop and voltage drop as a function of current with the power off (upper curve) and on (lower curve)

(b) Temperature drop as a function of power dissipation

Figure 12 - Plots of various characteristics of the TEC.

CAMERA ELECTRONICS DESIGN

In order to test the sensor in package, we used our in-house camera electronics, know as Compact, Reconfigurable, Camera Electronics (CoReCam). The electronics has the ability to provide biases, clocks and includes 14-bit ADCs for analog signal measurement. The biases and clocks are software configurable, and the timing patterns can be changed easily in the software. The electronics uses USB communication control for both control and video transmission, enabling simple control via a laptop. These electronics were integrated with the sensor, the TE-cooled package, a TEC controller and optics to the system shown in Figure 13. The lens used is a Stingray 25 mm lens with response from 0.48 to 2.5 μm .

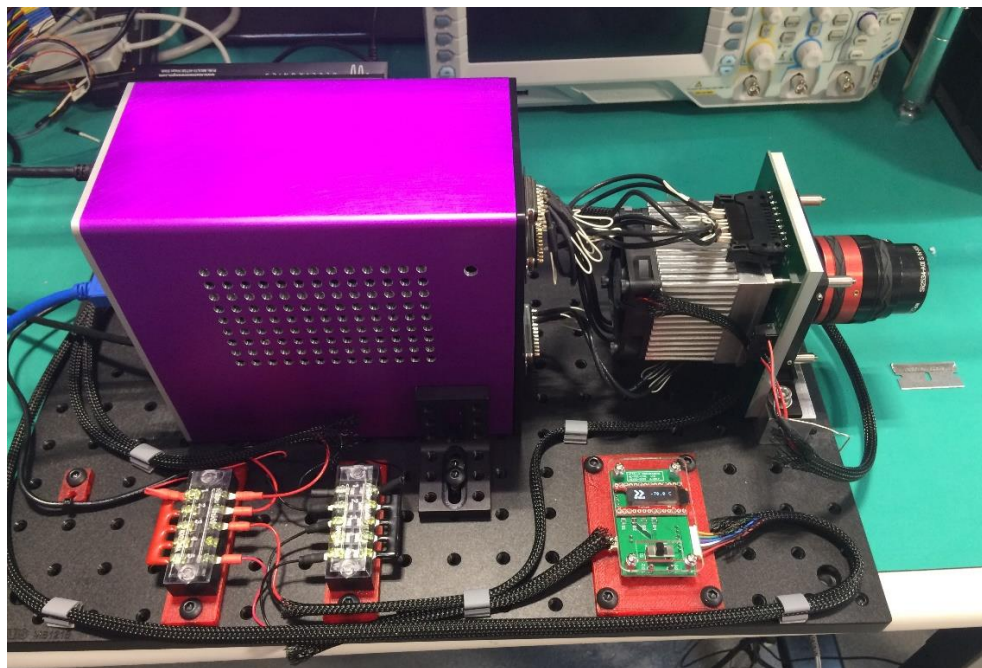


Figure 13 - Picture of full assembly with electronics, packaged sensor, TEC controller, and lens.

The integrated system was characterized by taking imagery. The same sensor as shown in Figure ??? was integrated into a TEC package and then integrated with the camera electronics. Using the 25 mm lens, outdoor imaging was performed, as shown in Figure 14. It showed similar characteristics to Figure 9, providing a clear indication that the packaging did not degrade the sensor.



Figure 14 - Outdoor imagery using structure 2 packaged in TEC, cooled to 208K.

In summary, the team was able to show a full system design, combining nBn material with a TE cooler and camera electronics to demonstrate an eSWIR system capable of operating without a cryocooler and the expense and other issues that come with it.

References

[1] Tennant, W. E., Donald Lee, Majid Zandian, Eric Piquette, and Michael Carmody. "MBE HgCdTe Technology: A very general solution to IR Detection, Described by "Rule 07", a very convenient Heuristic," *Journal of Electronic Materials* 37(9), 1406-1410 (2008).